AIAA 82-4206

# The Symmetric Turbulent Wake of a Flat Plate

B. R. Ramaprian* and V. C. Patel†
*University of Iowa, Iowa City, Iowa*
and
M. S. Sastry‡
*Avco Everett Research Laboratories, Everett, Mass.*

**Detailed measurements of mean flow and turbulence in the developing symmetric wake of a smooth, flat plate are presented. The results are discussed in the light of previous data and theories for near and far wakes. It is shown that evolution of the upstream boundary layers into the classical asymptotic wake occurs in three quite distinct stages and takes about 350 wake momentum thicknesses.**

## Nomenclature

$B$ = constant in logarithmic law = 5.5
$b$ = half-width of wake
$C_f$ = skin-friction coefficient = $\tau_w / \frac{1}{2}\rho U_\infty^2$
$E_1$ = exponential integral [Eq. (7)]
$G$ = nondimensional shear stress = $\tau/\rho W_0^2$
$G_{\max}$ = maximum value of $G$
$g$ = function defined by Eq. (8)
$H$ = shape parameter = $\delta_1/\delta_2$
$R_\delta^*$ = displacement-thickness Reynolds number = $U_\infty \delta_1/\nu$
$R_\theta$ = momentum-thickness Reynolds number = $U_\infty \delta_2/\nu$
$U$ = longitudinal mean velocity
$U_c$ = value of $U$ at wake centerline
$U_\infty$ = freestream velocity (constant)
$U_\tau$ = shear velocity in the boundary layer = $(\tau_w/\rho)^{1/2}$
$U_{\tau 0}$ = value of $U_\tau$ at trailing edge
$u$ = turbulent velocity in $x$ direction
$v$ = turbulent velocity in $y$ direction
$w$ = turbulent velocity along the span
$W$ = velocity defect = $U_\infty - U$
$W_0$ = maximum velocity defect = $U_\infty - U_c$
$x$ = downstream distance from trailing edge (distance from virtual origin in asymptotic growth and decay laws)
$y$ = coordinate normal to plate and wake centerline
$x^*$ = $U_{\tau 0}x/\nu$
$y^*$ = $U_{\tau 0}y/\nu$
$\gamma$ = Euler constant
$\delta$ = boundary-layer thickness
$\delta_1$ = displacement thickness $\left(= \int_{-\infty}^{\infty} \left(1 - \frac{U}{U_\infty}\right) dy$ for wake, $\int_0^\infty \left(1 - \frac{U}{U_\infty}\right) dy$ for boundary layer$\right)$
$\delta_2$ = moment thickness $\left(= \int_{-\infty}^{\infty} \frac{U}{U_\infty}\left(1 - \frac{U}{U_\infty}\right)$ for wake, $\int_0^\infty \frac{U}{U_\infty}\left(1 - \frac{U}{U_\infty}\right) dy$ for boundary layer$\right)$
$\delta_I$ = thickness of inner wake
$\eta$ = $y/b$
$\theta$ = momentum thickness in far wake or at last measurement station
$\kappa$ = Karman constant = 0.418
$\nu$ = kinematic viscosity
$\nu_T$ = eddy viscosity
$\rho$ = density
$\tau$ = Reynolds shear stress = $-\rho\overline{uv}$
$\tau_w$ = wall shear stress
$\zeta$ = $y/g$

Received Aug. 24, 1981; revision received Jan. 26, 1982. 

*Professor of Mechanical Engineering and Research Engineer, Iowa Institute of Hydraulic Research.
†Professor of Mechanical Engineering and Research Engineer, Iowa Institute of Hydraulic Research. Member AIAA.
‡Scientist.

## Introduction

It is well known that, even in the absence of flow separation, the pressure distribution over the rear of streamlined bodies is dictated by the interaction between the boundary layer, the wake, and the external flow. Hence, successful prediction of the performance of bodies such as airfoils, turbine and compressor blades, and underwater and surface vessels requires a knowledge of the flow in the so-called near wake and capabilities to continue boundary-layer-type solutions into that region. On the other hand, the structure of the asymptotic plane and axisymmetric turbulent far wakes has been well described by very simple classical theories. There are also excellent experimental data available on asymptotic two-dimensional turbulent wakes, e.g., Townsend.[1] These data were obtained mostly in wakes behind round cylinders, although other wake generators, such as square cylinders and twin plates,[2,3] have also been studied. In all these experiments, however, measurements were made only in the asymptotic wake, very far downstream (often several hundred characteristic body widths) of the body. They do not, therefore, provide any information on the evolution of the flow into the asymptotic state. This evolution may be quite different for different wake generators, even for nonseparating streamlined bodies, such as flat plates and airfoils at small incidences. However, in spite of the practical significance of such wake flows, fundamental studies in this area are relatively recent and somewhat limited.

By far the best-documented case is the simplest one, namely, the flow behind the flat plate at zero incidence. Here the viscous-inviscid interaction is very weak and the wake is two-dimensional, symmetric, and straight. This flow was studied experimentally by Chevray and Kovasznay[4] in 1969. Their experiments were practically the only source of data on such flows until recently, when additional experiments were reported by Andreopoulos[5] and Pot.[6] These three experiments differed from one another primarily in the quantities that were measured, the streamwise extent over

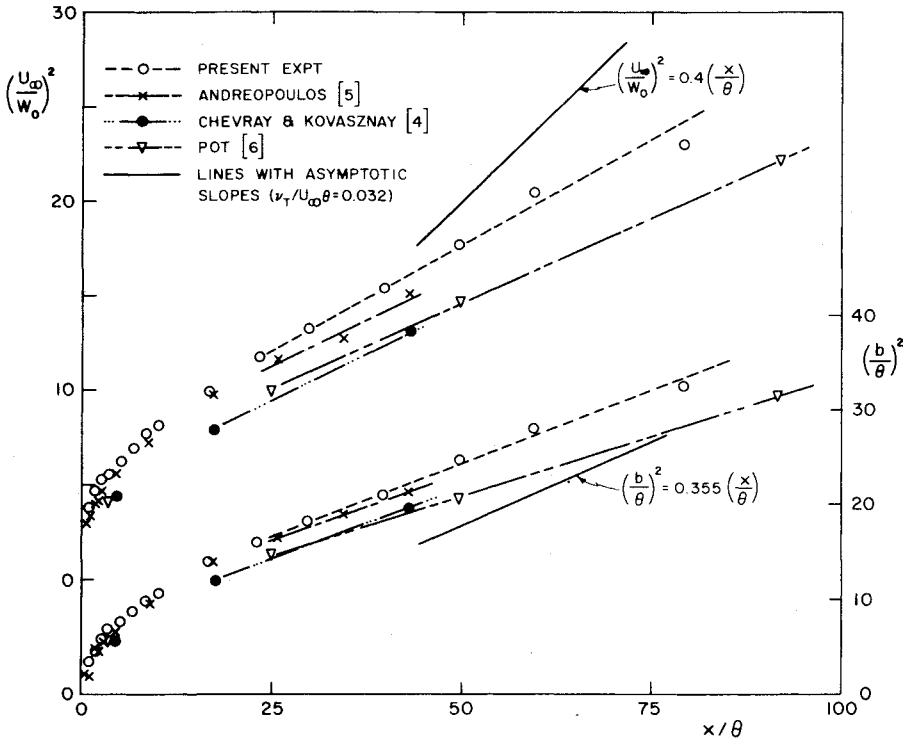


**Fig. 1 Near-wake development in similarity coordinates.**

which the data were obtained, and the state of the boundary layer at the trailing edge.

One of the interesting and important issues that arise in the discussion of wake development is concerned with the downstream distance from the trailing edge beyond which the wake can be regarded as having reached an asymptotic state. Associated with this issue is the labeling of the wake as "near wake" and "far wake." Intuitively, the wake can be said to have reached an asymptotic far-wake state if all flow properties, both mean and turbulent, attain universal distributions independent of the trailing-edge conditions. In practical applications, such as drag evaluation, however, it is sufficient to know the distance beyond which the mean-flow properties, such as velocity and pressure, reach universal distributions and the growth of the wake half-width $b$ and decay of maximum wake defect $W_0$ exhibit asymptotic trends, namely,

$$b \propto x^{1/2} \qquad W_0 \propto x^{-1/2} \tag{1}$$

where $x$ is the distance from a virtual origin. At the time the present study was initiated, the only available data of Chevray and Kovasznay[4] indicated that the mean-velocity profiles very nearly attained the theoretical universal asymptotic distribution within $x/\theta \sim 25$, where

$$\theta = \int_{-\infty}^{\infty} \frac{U}{U_\infty}\left(1 - \frac{U}{U_\infty}\right) dy$$

is the wake momentum thickness, $U$ the longitudinal mean velocity, and $U_\infty$ the constant freestream velocity outside the wake. Their data also indicated linear variations of $b^2$ and $1/W_0^2$ beyond this point, as suggested by Eq. (1). It was therefore concluded that the region $x/\theta < 25$ could be regarded as "near wake" and the rest as "far wake," at least from mean-flow considerations. When the data of Andreopoulos became available, they also indicated that mean-velocity profiles attained universal distributions beyond $x/\theta = 25$. But it was surprising to find that, although $1/W_0^2$ and $b^2$ each exhibited nearly linear variations with $x/\theta$ beyond $x/\theta = 25$ and up to the last measurement station at $x/\theta = 40$, their slopes were different from those measured by Chevray and Kovasznay. This can be seen from Fig. 1, which includes these and other, more recent data. Since it was inconceivable that two flat plate wakes could have different asymptotic growth rates, the differences were attributed, at the time, to errors in measurement. The experiments reported below were therefore planned to obtain a new set of accurate wake data in the range $0 < x/\theta < 80$. Based on the information available, it was assumed that this range would be more than sufficient to include the near- and far-wake regions. The experimental data, however, indicated yet another set of slopes for the growth/decay rates! Finally, the data of Pot[6] became available, which only increased further the scatter in Fig. 1. Pot's data are unique insofar as they extend to a large distance from the trailing edge, i.e., $x/\theta = 960$. These data showed that asymptotic growth rates are indeed attained, but only at distances much farther downstream than was studied in the other experiments, including the present one. This aspect will be discussed later in this paper. It is necessary to mention here only that these observations provided the motivation for this study of the stages in evolution of the developing wake.

This brief review indicates that, in spite of the numerous investigations noted above, a clear picture of the various stages in evolution of an asymptotic wake from the trailing-edge boundary layers has not emerged. This is the subject of the present paper. The paper is concerned primarily with the wake of a flat plate, with all its attendant simplifying features. First, a new set of data is presented. All available experimental evidence is then reviewed in the light of the well known properties of the asymptotic or far wake and the theories for near wakes to identify three distinct zones of wake development.

## Experiments

The experiments were carried out in the 1.6-m × 1.6-m closed-circuit wind tunnel of the Iowa Institute of Hydraulic Research. The length of the test section is 7.62 m. False walls were introduced in the octagonal test section, thus making it rectangular, as shown in Fig. 2. Freestream turbulence in the tunnel was less than 0.5%, and all measurements were made with a nominal speed of 22 m/s in the working section.

A 1829-mm-long × 635-mm-wide plate was constructed from a 19-mm plywood sheet sandwiched between two 1.5-

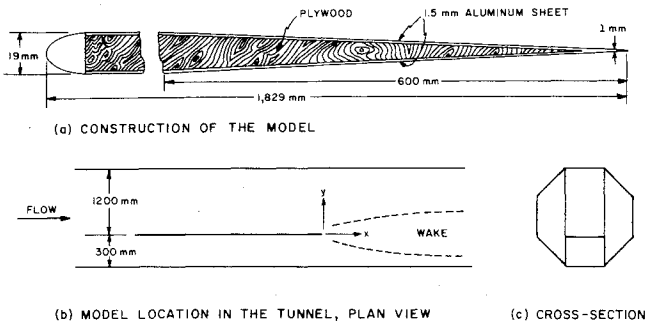


**Fig. 2 Construction and location of model.**

mm aluminum sheets stretched and glued together. The nose was rounded to a 1:2 elliptical shape. The last 670-mm length of the model was tapered at an included angle of 0.9 deg, and the last 50 mm was filed to terminate in a trailing edge of 1-mm nominal thickness. Figure 2a shows the details of construction. Strips 150 mm wide of 20-grade sandpaper were glued at a distance of 300 mm from the leading edge on both sides of the plate to promote early boundary-layer transition. The width, grade, and location of the sandpaper were selected after several trials so as to yield a "standard," fully turbulent, zero-pressure-gradient boundary layer upstream of the trailing edge.

The model was mounted vertically in the tunnel as shown in Figs. 2b and 2c. The off-centered mounting of the model was selected to limit the length of the probe support. Pitot and hot-wire traverses across the boundary layer and wake were carried out by a mechanized traverse that could be mounted anywhere along the side wall. The traverse was operated by a servocontrolled stepper motor and had a range of 20 cm and an accuracy of 0.025 mm. The coordinate system used to report the subsequent measurements is shown in Fig. 2b.

An extensive survey indicated no variation of static pressure along or across the wake. Mean velocities were measured with a total-head tube of 0.71 mm o.d., along with a static pressure probe located outside the wake. The skin-friction coefficient in the boundary layer was measured using the total-head tube as a Preston tube. Turbulence measurements were made using single- and $x$-wire probes of standard design, a dual-channel DISA hot-wire anemometer, a DISA correlator (which served as an add/subtract unit), and a four-quadrant multiplier. The instantaneous velocity products were time-averaged using a voltage-to-frequency converter followed by a bidirectional frequency counter. Hot-wire measurements also served as a check on the total-head measurements. The analog data processing method was verified in detail against a digital method developed for a later series of experiments. Details of these comparisons as well as those pertaining to various aspects of instrumentation, such as calibration and linearization, are discussed at length in Ref. 7. It suffices to mention that errors due to the use of unlinearized signals are negligible for the data reported here. The estimated uncertainties in the principal measurements are as follows: mean velocity $\pm 0.5\%$, rms turbulence intensities $\pm 2\%$, Reynolds shear stress $\pm 5\%$.

The boundary layer upstream of the trailing edge was fully developed and symmetrical. The skin-friction coefficients on the two sides of the plate agreed within 4%. The characteristic boundary-layer parameters (practically identical on both sides of the plate) at a station 76.2 mm upstream of the trailing edge were $\delta = 34$ mm, $R_\delta^* = 6790$, $R_\theta = 5220$, $H = 1.29$, and $C_f = 0.0029$. The mean-velocity distribution in the boundary layer at this station exhibited the standard logarithmic distribution in the wall region, i.e.,

$$U/U_\tau = 1/\kappa \ell n U_\tau y/\nu + B \qquad (2)$$

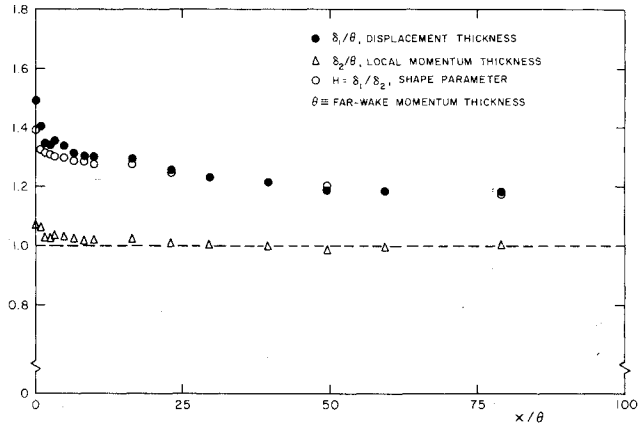


**Fig. 3 Integral parameters along the wake, present experiment.**

with the generally accepted values of $\kappa = 0.418$ and $B = 5.5$. The maximum wake defect $\Delta U_{max}/U_\tau$ for this profile was found to be 2.7, which is in reasonable agreement with the accepted value for a fully developed turbulent boundary layer at this Reynolds number. The distributions of the Reynolds stresses $\overline{u^2}$, $\overline{v^2}$, and $\overline{uv}$ were also measured at this station and compared with the data of Klebanoff.[8] Again, generally good agreement was indicated between the two sets of data. Details of all these comparisons are provided in Ref. 7. From these results it was concluded that the boundary layer at the trailing edge was in a state of equilibrium and that the mild taper near the trailing edge had no significant effect on flow development. Also, the measurements at this station provided adequate initial conditions for calculations of the wake.

All measurements were made along the midspan of the plate (the centerplane of the tunnel). The ratio of plate width to wake thickness was approximately 9, therefore good two-dimensionality of the flow was ensured. Nevertheless, checks for two-dimensionality were made by measurements in planes 150 mm above and below the centerplane at two $x$ stations, namely, 127 and 609.6 mm. Excellent agreement was observed among the measurements at the three spanwise stations with respect to the mean-velocity and Reynolds-stress distributions. Also, measurements of $\overline{uw}$ showed that the correlation between $u$ and $w$ was very small, indicating absence of streamline divergence. Again, details of these measurements are documented in Ref. 7.

## Results and Discussion

All experimental results are tabulated and discussed in Ref. 7. Here we shall present only those data that are relevant to the general theme of the paper.

Mean-velocity profiles were measured at 16 stations ranging from $x = 0$ to 609.6 mm. Streamwise development of the important integral parameters is shown in Fig. 3. It is observed that both the displacement thickness $\delta_1$ and the shape factor $H$ decrease continuously along the wake. The effect of finite thickness of the trailing edge, and hence possible local flow separation, is observable as a jump in $\delta_2/\theta$ (where $\delta_2$ is the local momentum thickness and $\theta = 7.7$ mm the momentum thickness at the last measuring station in the wake) near the trailing edge from the ideal value of 1 to about 1.07. The value recovers quickly to unity and remains essentially constant downstream (the variation being less than $\pm 2\%$), indicating the two-dimensionality of the flow and the absence of any longitudinal pressure gradients in the tunnel.

### Inner Wake

Bradshaw[9] used dimensional arguments to propose that the velocity distribution in the immediate vicinity of the trailing edge should scale with the velocity and length scales of the

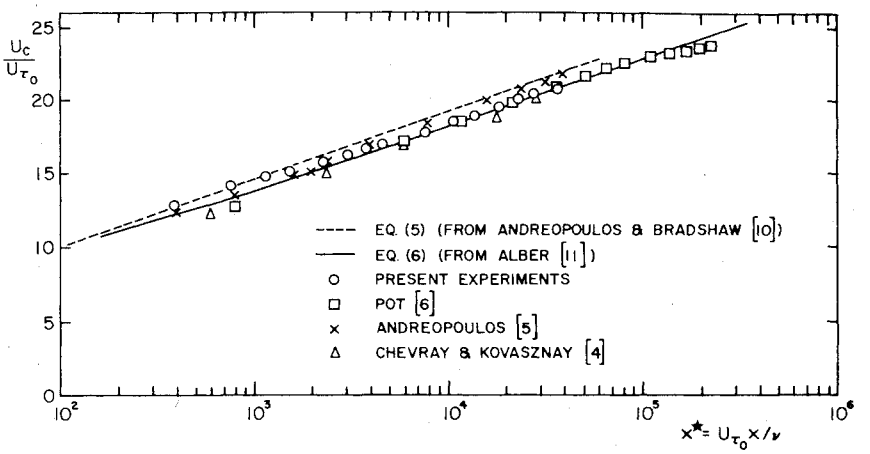


**Fig. 4 Development of centerline velocity.**

inner layer of the upstream boundary layer, namely,

$$U/U_{\tau 0} = f_1(U_{\tau 0}x/\nu, y/x) \qquad U_c/U_{\tau 0} = F_1(U_{\tau 0}x/\nu) \tag{3}$$

where $U_{\tau 0}$ is the shear velocity at the trailing edge and $U_c$ the centerline (minimum) velocity. The region in which Eq. (3) applies will be gradually destroyed by the spreading of what may be regarded as an "inner wake." Bradshaw estimated the extent of the inner wake by considering propagation of the disturbance created by the surface discontinuity at the trailing edge. Since the maximum width of the inner wake $\delta_1$ may be assumed to be equal to the thickness of the inner layer of the upstream boundary layer, say, $0.1\delta$, and Bradshaw's hyperbolic turbulence model indicates the lines of propagation of the disturbance to be inclined at an angle of about $0.55U_{\tau 0}/U_\infty$ to the axis, the lateral ($\delta_1$) and longitudinal ($x_1$) extents of the inner wake are

$$\delta_1/\delta \simeq \pm 0.2 \qquad U_{\tau 0}x_1/\nu \simeq 0.20U_\infty \delta/\nu \tag{4}$$

For typical values of $U_{\tau 0}/U_\infty$, this represents the region $x/\delta < 5$ or $x/\theta \simeq 25$. An attempt has been made to verify this proposition. Figure 4 shows the special case of the centerline velocity. On the basis of their own data, Andreopoulos and Bradshaw[10] suggested the empirical relation

$$U_c/U_{\tau 0} = 2.02 \ln x^* + 0.7 \tag{5}$$

where $x^* = U_{\tau 0}x/\nu$. Other data also indicate an approximate logarithmic growth of $U_c$, although some scatter is present.

The above arguments essentially ignore any influence of the sublayers of the upstream boundary layers. More recently, Alber[11] presented an analytical solution for the inner wake in two parts. In the central portion of the wake immediately downstream of the trailing edge, the flow is assumed to be laminar, and the well-known Goldstein solution is recovered. The thickness of this laminar inner wake grows as $x^{1/3}$, and the centerline velocity increases as $x^{1/3}$; the solution is valid until the inner wake grows to equal the upstream sublayer thickness. The streamwise extent of this region is approximately 10 sublayer thicknesses (say, $x^* < 100$) and is therefore very short. Downstream of this region, a turbulent inner wake develops into the initial logarithmic layer. Under the assumption of a linear eddy viscosity variation across the layer (which is rather unrealistic) and the existence of a similarity solution, the centerline velocity and the velocity distribution are given by

$$U_c/U_{\tau 0} = (1/\kappa)[\ln g(x^*) - \gamma] + B \tag{6}$$

$$U/U_{\tau 0} = (1/\kappa)\ln y^* + B + (1/\kappa)E_1(\zeta) \tag{7}$$

where

$$y^* = \frac{U_{\tau 0}y}{\nu}, \quad \zeta = y/g(x), \quad E_1(\zeta) = \int_\zeta^\infty \frac{e^{-t}}{t}\,dt$$

the function $g$ is defined by

$$g(\alpha)\{\ln g(\alpha) - 1\} = \kappa^2\alpha \tag{8}$$

and $\gamma$ ($=0.5772157$) is the Euler constant. Equations (6) and (7) were evaluated with $\kappa = 0.418$ and $B = 5.5$. The results for Eq. (6) are compared with all available data in Fig. 4. It is evident from this figure that Alber's theory shows good agreement with the present data and those of Pot.[6] Figure 4 also provides qualitative support for the purely empirical correlation of Andreopoulos and Bradshaw,[10] namely, Eq. (5).

Alber compared his solutions only with the data of Chevray and Kovasznay using $\kappa = 0.41$, $B = 5.0$, and the same value of $U_{\tau 0}$ as used in the present study, and showed better agreement between theory and experiment than depicted in Fig. 4. This indicates that the solution is quite sensitive to the values of $\kappa$ and $B$. A reanalysis of the Chevray and Kovasznay boundary-layer data using a Clauser plot confirmed that the present set of values, $\kappa = 0.418$, $B = 5.5$, are more appropriate for this flow. Hence, it is concluded that the small discrepancy between theory and experiment seen in Fig. 4 is genuine. It is, however, small, and surprisingly so for a theory based on an unrealistic eddy viscosity distribution. Further, it is worth mentioning that the centerline velocity $U_c$ is predicted quite well by Eq. (6) even beyond the near wake (in fact, up to $x^* \sim 30{,}000$), although the assumptions of Alber's theory are no longer valid. This is somewhat perplexing and suggests that Alber's theory requires further study. Figure 5 shows a comparison of Eq. (7) with the present data. The growth of the turbulent inner wake and gradual destruction of the log layer of the upstream boundary layer can be clearly seen from this figure. It is observed that the log layer is fully "consumed" by the inner wake in about $x/\theta = 25$. This result corresponds to an $x^*$ value of about 10,000 in the present experiments, as shown in the figure. This value for $x^*$ will of course increase with Reynolds number. One can conclude that, beyond this region, the wake is not directly influenced by the wall layer of the upstream boundary layer and hence it behaves as a free turbulent shear layer. We now designate the region $x/\theta < 25$ the "near-wake" region. The end of the near-wake region does not, however, mark the end of wake development or the beginning of the asymptotic wake that is discussed in the next section.

### Asymptotic Wake

The assumptions of self-preservation and small velocity defect in the wake lead to the well-known half-power laws for

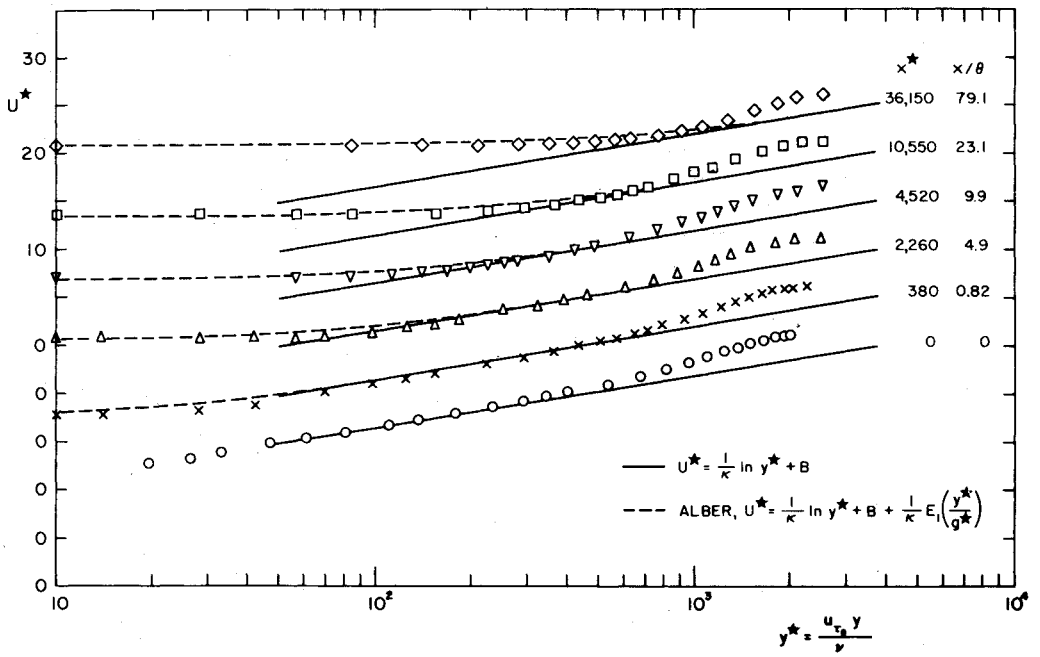


**Fig. 5 Velocity profiles in inner-layer coordinates, present experiment.**

the half-width $b$ and maximum velocity defect $W_0$ introduced earlier, in Eq. (1). If it is further assumed that the eddy viscosity $\nu_T$ is constant across the wake,[12] the shear-stress ($\tau$) and velocity defect ($W$) profiles are given by

$$G = \tau/\rho W_0^2 = 8(\ell n 2)\,(\nu_T/W_0 b)\,\eta \exp\{-4\eta^2 \ell n 2\} \tag{9}$$

$$F = W/W_0 = \exp\{-4\eta^2 \ell n 2\} \tag{10}$$

where $\eta = y/b$. Introduction of the wake momentum thickness $\theta$ leads to explicit growth and decay laws of the form

$$(b/\theta)^2 = 16(\nu_T/U_\infty \theta)\ell n 2\,(x/\theta) \tag{11}$$

$$(U_\infty/W_0)^2 = 4\pi(\nu_T/U_\infty\theta)\,x/\theta \tag{12}$$

so that

$$W_0 b/U_\infty \theta = (4\ell n 2/\pi)^{1/2} = 0.9394 \tag{13}$$

and is therefore independent of Reynolds number $U_\infty\theta/\nu_T$.

From some early results from the wakes of cylinders, Schlichting[12] deduced a value of 0.0444 for $\nu_T/U_\infty\theta$. Townsend,[1] however, quoted a value of 0.032, which is identical with the average value deduced from the more recent asymptotic wake data of Narasimha and Prabhu.[13] With this value for the eddy viscosity, the above equations imply that $G_{max}$ [the maximum value of $G$ in Eq. (9)] should approach 0.0487 in the far wake. The above results may be approximate because they are based on the assumption of constant eddy viscosity, but they are nevertheless adequate to serve as a basis for comparison between data obtained in far wakes originating from different initial conditions and for study of the approach to asymptotic conditions.

#### Behavior of the Mean Flow beyond the Near Wake

The behavior of the mean-flow properties in the wake beyond $x/\theta = 25$ can now be compared with the asymptotic behavior represented by the above results. Figure 6 shows some mean-velocity profiles in the wake. Data presented in this figure include typical results from the present experiments and those of Pot.[6] Also shown is the asymptotic profile given by Eq. (10). It is seen that the measured profiles agree well with the asymptotic profile for $x/\theta \geq 25$, except for a small discrepancy near the outer edge. It is also seen that for $x/\theta < 25$ the velocity profiles deviate substantially from the

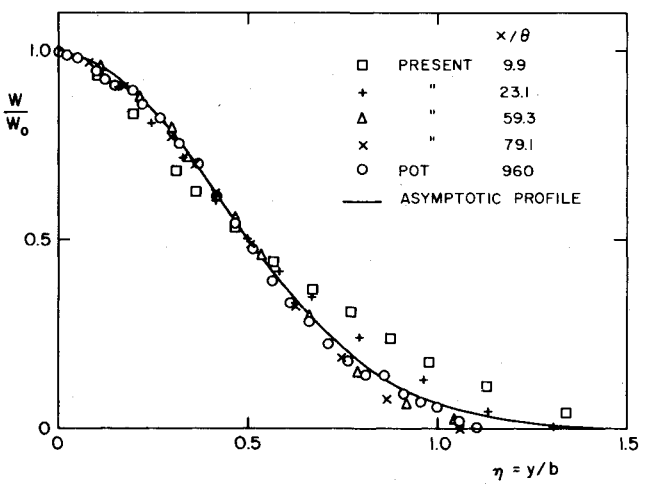


**Fig. 6 Velocity defect profiles in far-wake coordinates.**

asymptotic profile. Also, the results of Pot for $x/\theta = 960$ confirm that the wake would indeed eventually attain the profile given by Eq. (10). Figure 6 thus *appears* to indicate that the end of the near-wake regime at $x/\theta = 25$ marks establishment of a near-asymptotic mean-velocity profile in the wake; however, a study of the data on rate of growth of the scales of velocity and length in the wake leads to a different conclusion.

The streamwise developments of the length and velocity scales of the wake are shown in Fig. 1, which was introduced earlier. Figure 7 is an extension of this figure plotted to a scale that can accommodate the larger $x/\theta$ range studied by Pot. Figures 1 and 7 also show lines corresponding to Eqs. (11) and (12) with $\nu_T/U_\infty\theta = 0.032$. It is clear from these two figures that the centerline velocity defect and wake width do not follow the asymptotic power laws until about $x/\theta = 350$ and that the measurements at the most downstream station in the present experiment, as well as those of Chevray and Kovasznay and Andreopoulos, do not show asymptotic behavior. Only the measurements of Pot extend well into the asymptotic range as judged by these criteria. In other words, the end of the near-wake region at $x/\theta = 25$ does not signify that the wake has attained an asymptotic state even with respect to mean-flow behavior. Figure 7 also shows the variation of maximum shear stress $G_{max}$ with $x/\theta$. It is seen

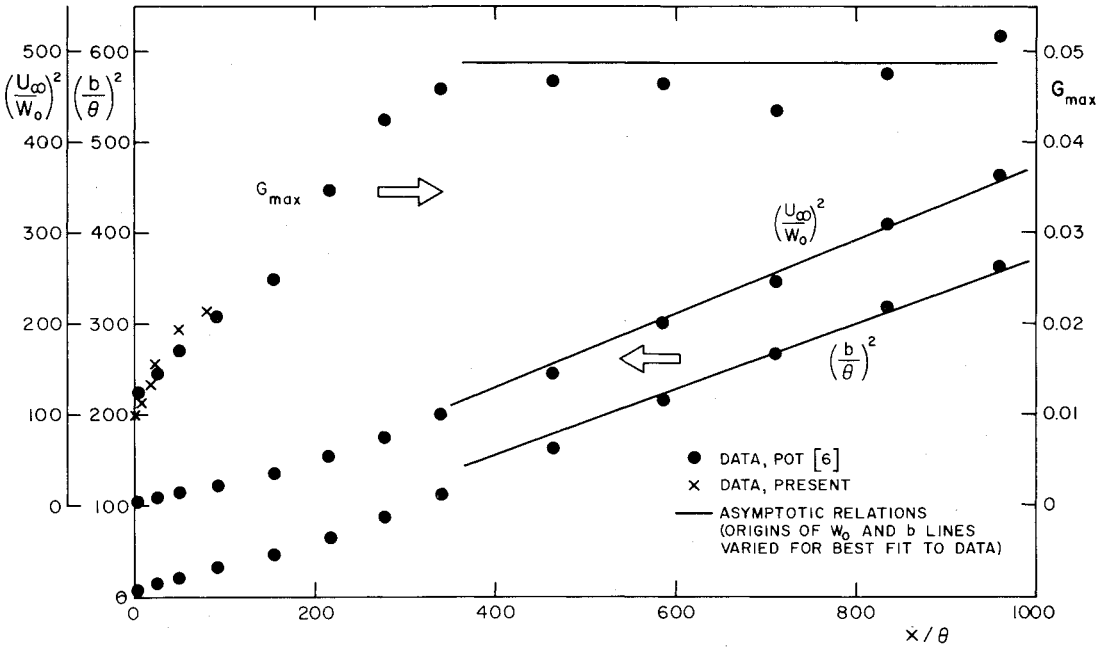


**Fig. 7 Approach to asymptotic growth and decay laws.**

that the present data are lower than the asymptotic value of 0.0487 even up to the last measurement location. Also shown in this figure are the data of Pot. These indicate that $G_{max}$ increases continuously with $x$ and approaches the asymptotic value only for $x/\theta \geq 350$.

#### Turbulence Structure in the Wake

Figures 8a, b, and c, respectively, show typical distributions of rms turbulence intensities $u'$ and $v'$ and Reynolds shear stress $\overline{uv}$ obtained from the present experiments. Since the symmetry of the flow was checked and confirmed, data for one-half of the wake only are presented. Also, the rms turbulence intensities $w'$ are not shown.

Perhaps the most unusual feature of these measurements is the presence of marked overshoots in the distributions of the shear stress $\overline{uv}$ and the normal velocity fluctuations $\overline{v^2}$ at the first few stations near the trailing edge. Very close to the trailing edge, the maximum value of $\overline{uv}$ exceeds that in the upstream boundary layer by a factor of more than 2. Such overshoots have been predicted by some calculations. However, it is believed that in the present case the overshoots are associated primarily with flow separation or vortex shedding behind the trailing edge of finite thickness. The trailing edge of the plate used in the present experiments was about 1 mm thick. Similar overshoots in the Reynolds-stress distributions are also present in the data of Pot, who used a plate of trailing-edge thickness comparable to that in the present case. The overshoots disappear beyond a distance of about 200 trailing-edge thicknesses. It is, however, easy to infer from the profiles in Figs. 8a-c that the turbulent structure is drastically different from the far-wake structure everywhere in the region studied; for example, $\overline{u^2}$ and $\overline{v^2}$ are seen to be considerably different from each other at all the measurement stations. In the far wake these should be nearly equal. More quantitative evidence of departure from the far-wake structure is provided by Fig. 8c, showing the behavior of the shear stress.

Figure 9 shows a typical comparison of the measured distributions of shear stress with the asymptotic profile given by Eq. (9). The data include present measurements at the most downstream location, $x/\theta = 79$, and Pot's measurements at $x/\theta = 960$. It is seen that Pot's data are in satisfactory agreement with theory. This agreement also suggests that the assumption of constant eddy viscosity in the far wake is reasonable. The discrepancy observed near the outer edge of the wake is possibly due to the intermittent structure of turbulence in this region. Similar conclusions should result from a study of the normal-stress components $\overline{u^2}$, $\overline{v^2}$, and $\overline{w^2}$, since their distributions should also be universal and their scales (e.g., the maxima or the centerline values) constant at large distances from the body, regardless of initial conditions. It appears that the data of Pot satisfy these requirements also for $x/\theta \geq 350$.

In summary, the available data, including those from the present experiments, indicate that the near-wake region $x/\theta \leq 25$ is followed by a very long region of further development before the wake approaches an asymptotic state in mean- and turbulent-flow properties. Pot's data indicate that the asymptotic state is attained beyond $x/\theta \simeq 350$. The developing region between $25 \leq x/\theta \leq 350$ can be called the "intermediate wake." The characteristics of this region will be examined next in more detail.

#### Intermediate Wake and Local Similarity

Prabhu[3] observed that a developed asymptotic wake recovering from a disturbance, such as a sudden pressure gradient, exhibits local similarity in the distributions of the Reynolds stresses; that is, when normalized by local length and velocity scales, the Reynolds-stress distributions are self-similar. The mean-velocity profiles in the intermediate wake exhibit this type of similarity, as shown earlier by the data presented in Fig. 6. The behavior of the turbulent properties is seen from Fig. 10, which shows the distributions of shear stress using the local maximum value and wake half-width as normalizing scales at several locations in the range $x/\theta > 25$. Data from different experiments are included in this figure. The shaded area represents the data of Prabhu.[3] It is seen that all the data, with the exception of those of Andreopoulos,[5] nearly collapse on one another. The departure of the data of Andreopoulos from this trend is more likely due to experimental errors. In fact, the data for the outer region of the wake, where this departure is seen, were not reported or used for discussion by Andreopoulos and Bradshaw.[10] The asymptotic far-wake shear-stress distribution $G(\eta)$, normalized with $G_{max}$, is also shown in this figure. It is interesting to note that the resulting distribution coincides with the local similarity distribution in the inner part of the wake. Differences in the outer part are believed to be due to intermittency effects. Similar results were obtained with the three normal stresses, and turbulent kinetic energy, but are not shown here.

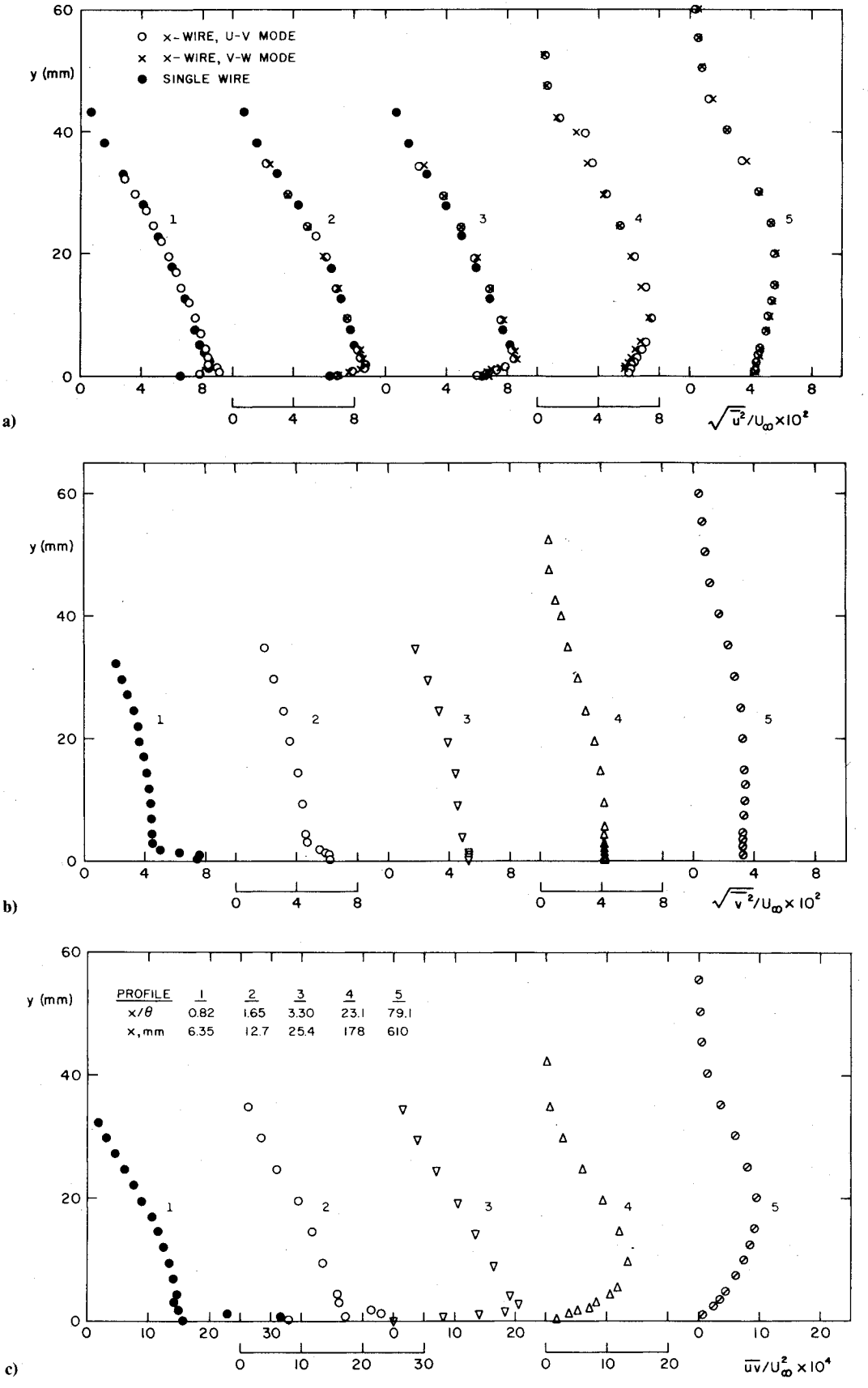


**Fig. 8 Typical Reynolds-stress distributions, present experiments.**

The observed local similarity suggests that, once the wake is out of the zone of influence of the wall layer, it develops into the asymptotic state in a universal manner, regardless of whether this development occurs after a disturbance or during natural evolution. Physically, this intermediate zone of development represents the region over which the large eddies in the outer parts of the initial boundary layer mix to form eventually a single asymptotic free shear layer.

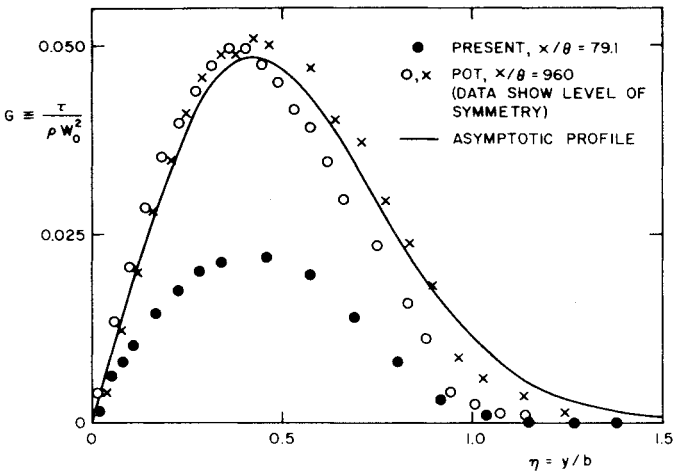


**Fig. 9 Approach to asymptotic stress profile.**

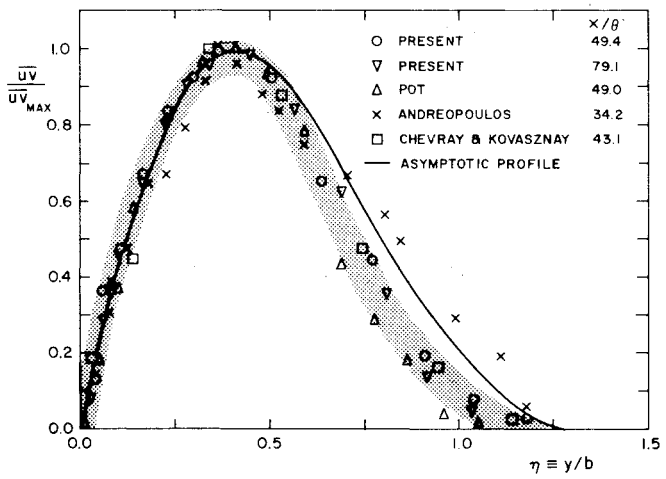


**Fig. 10 Local similarity of shear-stress profiles in the intermediate wake.**

## Conclusions

From the above observations, it is now possible to identify the various stages in development of the wake of a smooth flat plate.

The asymptotic state is reached at quite large distances ($x/\theta \gtrsim 350$) from the trailing edge. Beyond this distance, the turbulence structure becomes independent of the initial conditions and the growth rates are well predicted by classical far-wake analysis and such simple turbulence models as constant eddy viscosity.

The region between the trailing edge and the beginning of the asymptotic state may be called the "developing wake." This region can be further divided into two regions.

The first region, called the "near wake," is characterized by development of an inner wake and is the region influenced by the wall layer of the initial boundary layers. The rates of growth of $b/\theta$ and $U_\infty/W_0$ in this region are large compared with the asymptotic growth rates. The centerline velocity and the velocity distribution across the inner part of the wake can be adequately described by Alber's[11] analysis. The near wake extends from the trailing edge to $x/\theta \simeq 25$. The flow in the immediate neighborhood of the trailing edge is also influenced by the geometry and thickness of the trailing edge. This influence may be present over a distance of about 200 trailing edge thicknesses.

The next region, $25 < x/\theta < 350$, of the developing wake may be called the "intermediate" wake. In this region, influence of the upstream wall layers becomes insignificant and the wake evolves as a free turbulent flow. Local "similarity" of the mean-velocity and turbulence profiles is observed in this region. The intermediate wake is also characterized by slower rates of growth of the wake width and decay of the centerline defect than occur either in the near wake ($x/\theta < 25$) or in the far wake ($x/\theta > 350$).

In physical terms, the three zones of wake development may be described by the level of mixing between the two individual boundary layers at the trailing edge. The inner layer of the near wake is the region of small-scale mixing between the upstream wall layers. This mixing process has been studied in considerable detail in the experiments of Andreopoulos and Bradshaw.[10] Also in this region, mixing is confined to the inner wake, the outer velocity defect layers remaining practically unchanged. The intermediate wake is the region over which mixing occurs between the outer layers. The asymptotic state is reached when this mixing is completed. All memory of the boundary layers on the body is then destroyed. The dynamics of the large-scale mixing that determines evolution of the near wake into the asymptotic far wake have to be well understood in order to predict the flow in this regime with reasonable accuracy. To the authors' knowledge, the large-scale mixing in the intermediate zone of the wake has not been studied and would be worthy of future investigation.

## Acknowledgments

This study was supported by Grant NSG-2300 from the National Aeronautics and Space Administration, with Dr. J. G. Marvin as technical monitor. The authors also acknowledge many fruitful discussions with Dr. A. Prabhu.

## References

[1] Townsend, A. A., *The Structure of Turbulent Shear Flow*, Cambridge University Press, Cambridge, 1956.

[2] Kumar, P., "A Study of Wakes Behind Two-Dimensional Bodies," M.E. Dissertation, Dept. of Aeronautical Engineering, Indian Institute of Science, Bangalore, 1972.

[3] Prabhu, A., "Non-equilibrium Wakes," Ph.D. Thesis, Dept. of Aeronautical Engineering, Indian Institute of Science, Bangalore, 1971.

[4] Chevray, R. and Kovasznay, L.S.G., "Turbulence Measurements in the Wake of a Thin Flat Plate," *AIAA Journal*, Vol. 7, 1969, pp. 1641-1643.

[5] Andreopoulos, J., "Symmetric and Asymmetric Near-Wake of a Flat Plate," Ph.D. Thesis, Dept. of Aeronautics, Imperial College, London, 1978.

[6] Pot, P. J., "Measurements in a 2-D Wake and in a 2-D Wake Merging into a Boundary Layer," Data Report, NLR TR-79063 U, the Netherlands, 1979.

[7] Ramaprian, B. R., Patel, V. C., and Sastry, M. S., "Turbulent Wake Development Behind Streamlined Bodies," Institute of Hydraulic Research, University of Iowa, Iowa City, IIHR Rept. 231, 1981.

[8] Klebanoff, P. S., "Characteristics of Turbulence in a Boundary Layer with Zero Pressure Gradient," NACA Rept. 1247, 1955.

[9] Bradshaw, P., "Prediction of the Turbulent Near Wake of a Symmetrical Aerofoil," *AIAA Journal*, Vol. 8, 1970, pp. 1507-1508.

[10] Andreopoulos, J. and Bradshaw, P., "Measurement of Interacting Turbulent Shear Layers in the Near Wake of a Flat Plate," *Journal of Fluid Mechanics*, Vol. 100, 1980, pp. 639-668.

[11] Alber, I. E., "Turbulent Wake of a Thin, Flat Plate," *AIAA Journal*, Vol. 18, 1980, pp. 1044-1051.

[12] Schlichting, H., *Boundary Layer Theory*, 6th ed., McGraw-Hill, New York, 1968, pp. 685-694.

[13] Narasimha, R. and Prabhu, A., "Equilibrium and Relaxation in Turbulent Wakes," *Journal of Fluid Mechanics*, Vol. 54, 1972, pp. 1-17.